DOI: 10.21062/mft.2026.026 http://www.journalmt.com

3D Printing – Weight Optimization of FDM-Printed Components Using PLA and PETG

Alexandr Fales (0009-0008-0055-611X)[1], Vít Černohlávek (0000-0001-6816-1124)[1], Marcin Suszynski (0000-0001-7926-0574)[2], Jan Štěrba (0000-0002-2676-3562)[1], Patrik Balcar (0009-0007-4924-5681)[1], Marek Makúch (0009-0009-1338-4350)[3], Pavel Houška (0000-0003-4295-258X)[1]

[1]Faculty of Mechanical Engineering, J. E. Purkyne University in Usti nad Labem. Pasteurova 3334/7, 400 01 Usti nad Labem, Czech Republic. E-mail: alexandr.fales@ujep.cz, vit.cernohlavek@ujep.cz, jan.sterba@ujep.cz

[2]Faculty of Mechanical Engineering, Poznan University of Technology, Poland. E-mail: marcin.suszynski@put.poznan.pl

[3]Faculty of Industrial Technologies in Púchov, Alexander Dubček University of Trenčín. Ivana Krasku 1809/34, 020 01 Púchov, Slovak Republic. E-mail: marek.makuch@tnuni.sk

The aim of this study is to optimize the mass of FDM replicas of a selected part from VEX educational robotics kits (2×12 Beam, 228 2500 026) while maintaining functional compatibility for school use. Replicas were printed on an Original Prusa MK4 using PLA and PETG, with four infill patterns (Grid, Gyroid, Honeycomb, and Triangular) and infill densities of 15, 25, 40, 50, 60, and 70%. In total, 720 specimens were produced, and 15 original parts were used as a reference set. The reference mass of the original part was 11.349 ± 0.013 g. The mean mass of printed replicas increased with infill density; PLA specimens ranged from 12.590 to 16.361 g, while PETG specimens ranged from 12.996 to 16.855 g, depending on the selected pattern and density. At the same infill density, Gyroid generally showed lower mass values than Honeycomb. Functional compatibility was verified under secondary school conditions with respect to dimensional fit, connection reliability, and repeated assembly and disassembly in robotic constructions. Mechanical destructive testing was beyond the scope of the present study and will be addressed separately.

Keywords: 3D printing, PLA, PETG, Infill density, Educational robotics

1 Introduction

Additive manufacturing, particularly Fused Deposition Modeling (FDM), is among the most accessible and widely used technologies for producing polymer parts intended for prototyping, functional applications, and educational use. Its importance lies mainly in its technological simplicity, relatively low cost, broad availability of printing materials, and the ability to fabricate geometrically complex components without the need for specialized tooling [1–3]. Owing to these advantages, FDM is increasingly used not only for visual prototypes but also for the production of functional parts and replacement components intended for practical technical applications, where material selection and experimental verification play an important role [2,4].

Previous studies have repeatedly shown that the final properties of FDM-manufactured parts are determined not only by the geometry of the printed model, but also to a large extent by the selected material and the applied printing parameters [1,3,5]. The most influential parameters include print orientation, layer height, extrusion temperature, printing speed, number of walls, infill type, and infill density. These factors affect not only the mechanical performance of printed parts, such as strength, stiffness, and failure behavior, but also dimensional accuracy, surface quality, material consumption, printing time, and the final weight of the component [3,5–8].

From a practical point of view, PLA and PETG are among the most commonly used materials for FDM printing. PLA is widely employed because of its good printability, low warping tendency, and ability to provide stable results even on commonly available desktop printers. PETG, in contrast, is often selected for applications requiring higher toughness, better resistance to service loading, and lower brittleness while maintaining relatively good processability. A comparison of these two materials is therefore important not only from the perspective of laboratory testing, but also in practical applications where a compromise must be found between ease of manufacturing, mechanical response, stability, and final part weight [5,7–9].

A substantial part of the published research has focused on the effect of infill density and infill

topology on the mechanical properties of FDM prints. It has been repeatedly demonstrated that increasing infill density generally improves the strength and stiffness of printed parts, while the selected infill pattern modifies internal material distribution, load transfer, and local stress concentration. At the same time, different topologies, such as Grid, Gyroid, Honeycomb, Triangular, Concentric, or Cubic, may exhibit different mechanical responses even at the same nominal infill density. The selection of a suitable combination of infill density and infill pattern therefore represents an important step in optimizing the performance of FDM-manufactured components [5–8,10].

In addition to mechanical behavior, infill density and pattern also influence the amount of deposited material and, consequently, the final weight of the part. This parameter is important in practical applications not only from the perspective of material consumption and production economy, but also with regard to assembly behavior, inertia, structural stability, and the loading of drive elements. Although the literature describes in considerable detail the relationship between FDM process parameters and mechanical properties, less attention has been paid to studies that systematically evaluate the weight of functionally usable replicas of specific technical parts while simultaneously considering their operational compatibility [2,9].

This issue is particularly relevant in educational robotics and school-based technical practice, where lost or damaged original components often need to be replaced quickly and economically. In such cases, geometric similarity alone is insufficient; compatibility with the original construction system, repeated assembly and disassembly, and adequate robustness during routine use must also be ensured. At the same time, excessive part weight may negatively affect the behavior of the robotic assembly, for example in terms of stability, dynamic response, or motor loading [9].

This study also builds on the authors' previous research, which focused on the selection of suitable filament materials for 3D printing components of the VEX GO and VEX IQ construction systems with regard to mechanical properties, printability, and practical usability in school environments [4,11]. Based on those findings, PLA and PETG proved to be promising materials for further experimental evaluation. Following this outcome, the present study focuses on another important design variable, namely the effect of infill type and infill density on the final weight and functional compatibility of printed replicas.

The aim of this study is therefore to evaluate the weight and functional compatibility of FDM replicas of the VEX IQ 2×12 Beam (228-2500-026) manufactured from PLA and PETG using four infill patterns (Grid, Gyroid, Honeycomb, and Triangular) and six infill density levels (15, 25, 40, 50, 60, and 70%). The study seeks to quantify the effect of material selection, infill topology, and infill density on the final weight of the printed parts, while also verifying their practical usability in robotic assemblies under school conditions. In this way, the paper combines an experimental evaluation of FDM printing parameters with an application-oriented assessment of the usability of printed replicas in a real educational environment.

2 Materials and Methods

2.1 Studied part and reference samples

The studied part was a VEX IQ component 2×12 Beam (228-2500-026). The geometry of the investigated part is shown in Fig. 1, as the arrangement of holes and the slender beam-like shape are relevant for both material consumption and practical assembly compatibility. To determine the reference mass, 15 original parts were used. The experimental part consisted of FDM replicas printed from two thermoplas-tics: PLA and PETG. In total, 720 replicas were printed. The selected component represents a typical structural element frequently used in educational robotic assemblies and is therefore suitable for evaluating the practical applicability of printed replicas [9,11].

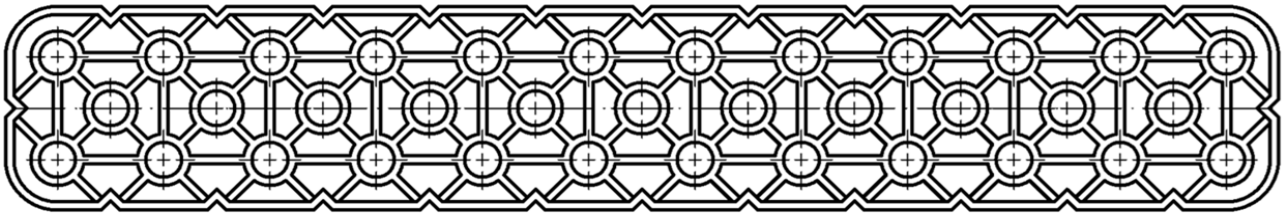

Fig. 1 *Reference part VEX Robotics 2×12 Beam (228-2500-026)*

2.2 Materials

Two commonly available FDM 3D printing materials were used to produce the replicas: PLA and PETG. The material selection reflects the requirements of school practice, especially the need for reliable printing without post-processing, particularly with respect to availability, stable printability, and sufficient mechanical properties for

functional parts. PLA was selected for its very good printability and low tendency to warp, which is suitable for rapid iterations and repeata-ble results in teaching. PETG was selected as a tougher alternative with higher resistance to operational loading while maintaining good printability when the printing process is properly set up [4,12].

In the experiment, Prusament (Prusa Research) filaments with a diameter of 1.75 mm were used (1 kg spools). To clearly distinguish samples among infill variants, the following colors were used; color served for sample identifi-cation only:

PLA (Prusament, 1 kg):

- Grid: Prusament PLA Galaxy Silver
- Gyroid: Prusament PLA Prusa Galaxy Black
- Honeycomb: Prusament PLA Galaxy Green
- Triangular: Prusament PLA Galaxy Red

PETG (Prusament, 1 kg):

- Grid: Prusament PETG Terracotta Light
- Gyroid: Prusament PETG Clear
- Honeycomb: Prusament PETG Jungle Green
- Triangular: Prusament PETG Lipstick Red

Filaments were stored in the laboratory storage facility at FSI UJEP (destructive testing laboratory) with monito-red temperature and humidity. Filament was removed from the original packaging only immediately before use in the 3D printer. Filament drying was not performed in this experiment, because the storage conditions and handling were set to minimize the risk of moisture uptake.

From the available infill patterns, four topologies were selected for printing replicas of VEX IQ parts intended for school use: Grid, Triangular, Honeycomb, and Gyroid. The selection was made with respect to practical use in school tea-ching (printing reliability, predictable behavior, print time, and material consumption) and expected mechanical behavior in typical structural applications. Gyroid is advantageous for multidirectional loading due to its conti-nuous 3D structure and good torsional and impact resistance. Honeycomb and Triangular provide high stiffness at the same mass, especially for plate-like and arm-type parts, and they also support top surfaces well. Grid was included as a fast and didactically clear option for prototyping and for demonstrating the effect of extrusion path orientation on resulting properties [4,13].

Brief characteristics of the selected infills:

- Grid (rectilinear, 0/90°): fast printing, more pronounced anisotropy; suitable for rapid prototypes and parts loaded mainly along the extrusion paths.
- Triangular: good stiffness to material ratio, better shear stiffness than Grid; suitable for parts requiring higher stiffness at low mass.
- Honeycomb: consistent printing, very good support of top surfaces; suitable for lightweight and stiff "panel type" parts.
- Gyroid (TPMS): continuous toolpaths, good torsional and shear behavior, higher resistance under mul-ti directional loading; suitable for structural parts with varying load directions.

For experimental verification, infill densities of 15, 25, 40, 50, 60, and 70 % were selected across all four topolo-gies. The range includes low values (15–25 %) for lightweight and time efficient configurations, mid range values (40–50 %) as a practical compromise for school operation, and higher values (60–70 %) to evaluate benefits at higher material fractions. Solid infill (100 %) was not included, because it leads to a disproportionate increase in mass and print time with relatively small additional benefit for typical school use and may increase the risk of internal defects and deformation [14-16].

2.3 Printing equipment and software

All replicas were printed on an Original Prusa MK4 3D printer. PrusaSlicer 2.9.4 was used for print preparati-on.

2.4 FDM printing settings (constant parameters)

For all prints, the 0.15 mm – Structural profile was used, with a 0.4 mm nozzle and a 0.15 mm layer height. The number of perimeters was set to 2. Printing was performed without supports, and the samples were left without post processing (i.e., without any additional finishing after printing). Other printing parameters were kept as de-fined by the selected PrusaSlicer profile to ensure repeatability and comparability among samples.

For PLA, nozzle temperatures of 210–215 °C and bed temperatures of 50–60 °C were used on a smooth PEI sheet without any adhesive agents. For PETG, nozzle temperatures of 240–250 °C and bed temperatures of 85–90 °C were applied on a satin sheet using 3DLAC as a separation/adhesion layer [13,17]. A complete overview of the printing parameters is provided in Table 1.

Tab. 1 *Printing and Material-specific parameters*

Parameter	Setting / value
3D printer	Original Prusa MK4
Printing location	FSI UJEP
Slicer	PrusaSlicer 2.9.4
Profile	0.15 mm – Structural
Technology	FDM
Nozzle diameter	0.4 mm
Nozzle material	Brass (standard)
Layer height	0.15 mm
Number of perimeters	2
Part orientation	Flat on the build plate
Supports	Not used
Post-processing	Not performed
Print speeds	Default PrusaSlicer profile for Original Prusa MK4 (no modifications)
Cooling (fan)	Default PrusaSlicer profile for the given material (no modifications)
Infill density (variable)	15 %, 25 %, 40 %, 50 %, 60 %, 70 %
Infill pattern (variable)	Grid, Triangular, Honeycomb, Gyroid
Specimens per combination	15 specimens (material × pattern × density)
Total printed specimens	720 pcs (PLA + PETG)
Original reference parts	15 specimens

Material-specific parameters				
Material	Nozzle temperature	Bed temperature	Build plate	Bed adhesion
PLA	210–215 °C	50–60 °C	Smooth PEI sheet	None (not used)
PETG	240–250 °C	85–90 °C	Satin sheet	3DLAC (spray)

2.5 Experimental design: factors and combinations

The experiment was designed as a full factorial study with the following factors:

- Material: PLA, PETG
- Infill pattern: Grid, Gyroid, Honeycomb, Triangular
- Infill density: 15, 25, 40, 50, 60, 70%

In total, 48 combinations were tested (2 × 4 × 6). For each material × pattern × density combination, 15 pieces were printed, i.e., 48 × 15 = 720 replicas. Examples of printed part replicas made of PLA and PETG are shown in Figures 2 and 3. The visual documentation of this condition is important for the transparency of the experiment, as it confirms that the measured mass values and their variability, determined using the GF 200 digital laboratory balance by HELAGO, correspond directly to the output of the FDM printing process and are not affected by any subsequent interventions in the geometry or surface of the part. At the same time, this approach reflects the conditions of school practice, where additional finishing operations would represent a time-consuming and difficult-to-standardize step [18-20].

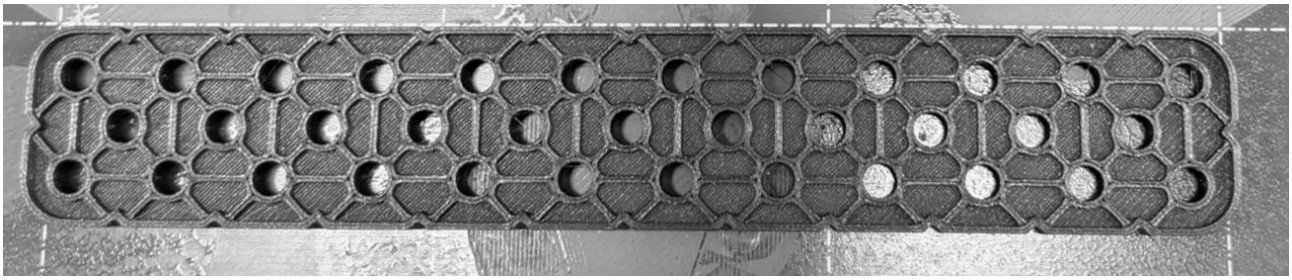

Fig. 2 *Printed structural element 2x12 Beam (228-2500-026) VEX – material used: PLA*

ISSN 1213–2489
e-ISSN 2787–9402

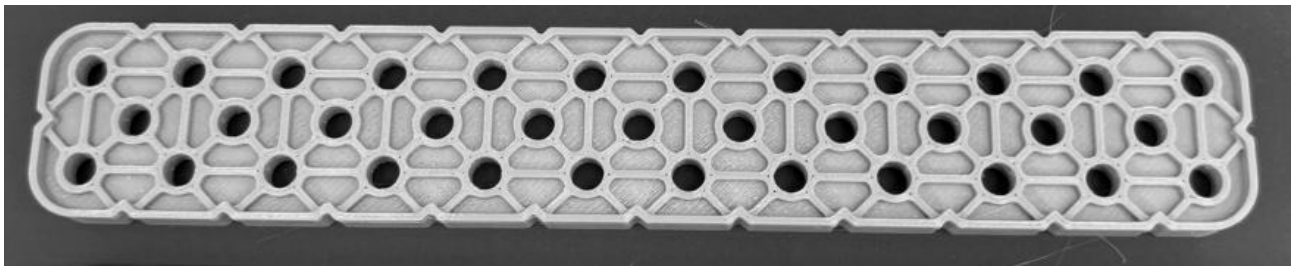

Fig. 3 *Printed structural element 2x12 Beam (228-2500-026) VEX – material used: PETG*

2.6 Mass measurement

The mass of the original parts and the printed replicas was measured for each piece individually using a GF-200 digital laboratory balance manufactured by HELAGO. The applied balance resolution was 0.001 g. Before measuring each set of 15 samples, a calibration was performed according to the manufacturer's instructions, followed by zeroing the scale. Measurements were carried out in an air-conditioned room on a stable surface and without drafts. The following environmental conditions were recorded during measurement: temperature 20.8–20.9 °C, air pressure 997.8–998.5 hPa, and relative humidity 34.8–35.1 %. Figure 4 documents the weighing setup used for the mass measurements and supports the transparency and repeatability of the measurement procedure.

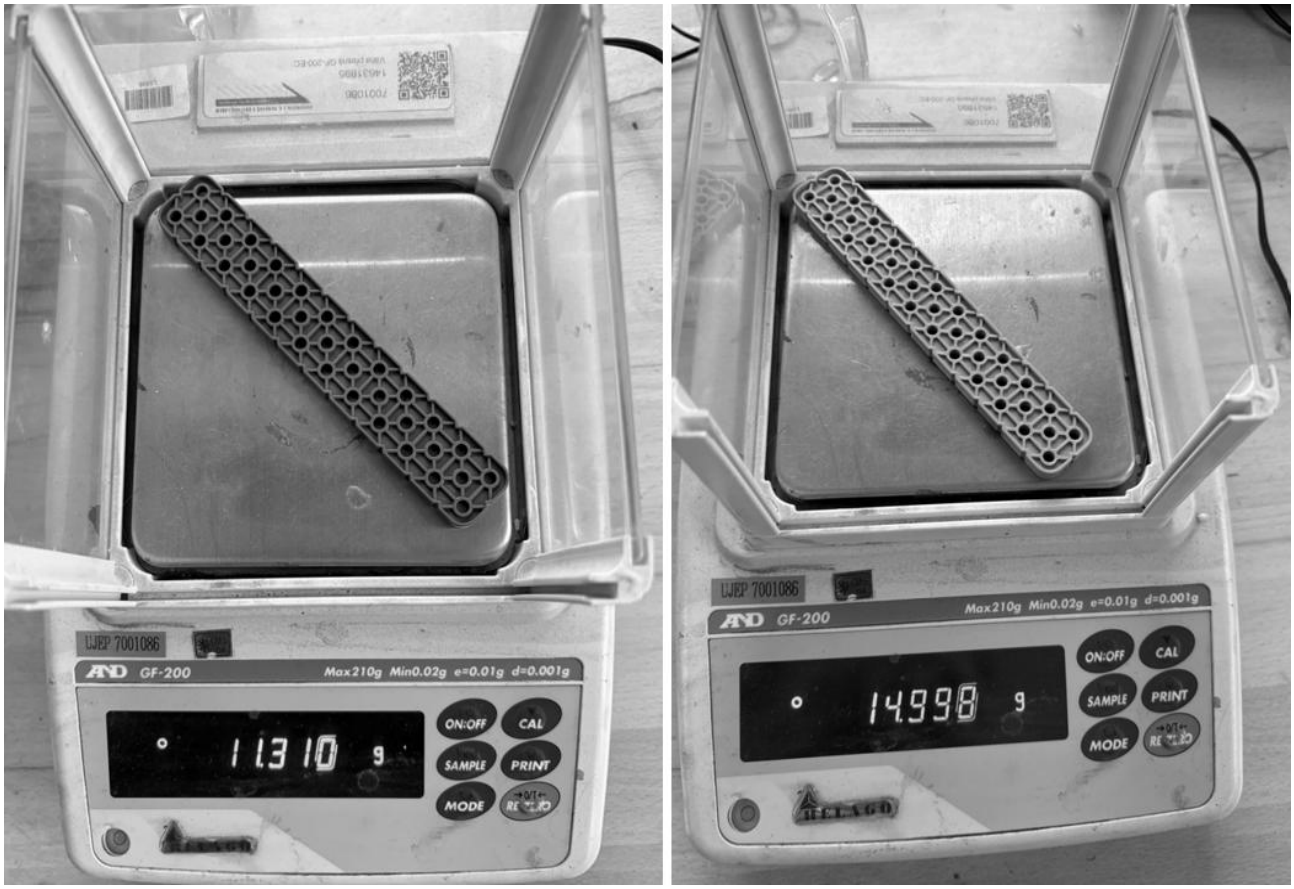

Fig. 4 *Measurement using a professional digital laboratory scale Helago GF-200*

2.7 Functional compatibility assessment

Functional compatibility of the replicas was assessed in a secondary-school environment during practical use in VEX IQ assemblies. The evaluation focused on fit with original components, joint reliability, and behavior under repeated assembly and disassembly in robotic builds. Destructive mechanical tests (e.g., tensile testing, bending) were not performed in this study and are planned as follow-up work.

2.8 Data processing and presentation

Measured values were aggregated by groups according to the experimental plan. For interpretation, differences between materials, the effect of infill pattern, and the mass trend as a function of infill

density were compared. Results are presented in tables and graphs of mean values with variability indicated.

3 Results

3.1 Reference mass of the original part

The reference mass of the original 2×12 Beam (228-2500-026) part was determined by measuring n = 15 pieces. The mean mass was 11.349 ± 0.013 g (standard deviation SD = 0.0128 g; rounded to 0.001 g). This value was used as the reference level m_0 for evaluating both the absolute and relative mass increase of the FDM replicas in Table 2.

3.2 Mass increase: definitions and evaluation approach

To directly compare the replicas with the original part, the following metrics were evaluated for each configuration (material × infill pattern × infill density):

- Absolute mass increase:

$$\Delta m = m - m_0 \quad (1)$$

- Relative mass increase:

$$\Delta m_r = \frac{m - m_0}{m_0} \cdot 100\% \quad (2)$$

Where:

m…The mean mass of a given replica group,

m_0…The mean mass of the original part (see Section 3.1).

In Table 2, masses are reported m as mean ± SD for n = 15 specimens per group.

3.3 Effect of infill density and infill pattern on the mass of PLA replicas

For replicas printed from PLA, a clear monotonic increase in mass with increasing infill density was observed across all investigated infill patterns (Grid, Gyroid, Honeycomb, Triangular) (Table 2). Already at the lowest density of 15%, mean masses ranged from 12.590 to 12.920 g, corresponding to approximately +10.9 to +13.8% relative to the original part. At 70% infill, masses reached 15.548–16.361 g, i.e., approximately +37.0 to +44.2% relative to the original.

When comparing infill patterns at the same density, Gyroid repeatedly appeared as the most mass-efficient option, whereas Honeycomb produced the highest masses (e.g., at 70%: Gyroid 15.548 g vs. Honeycomb 16.361 g; Table 2). Differences between patterns are smaller than the effect of changing infill density; however, in absolute terms they can still be practically relevant (on the order of tenths of a gram up to ~0.8 g, depending on the configuration).

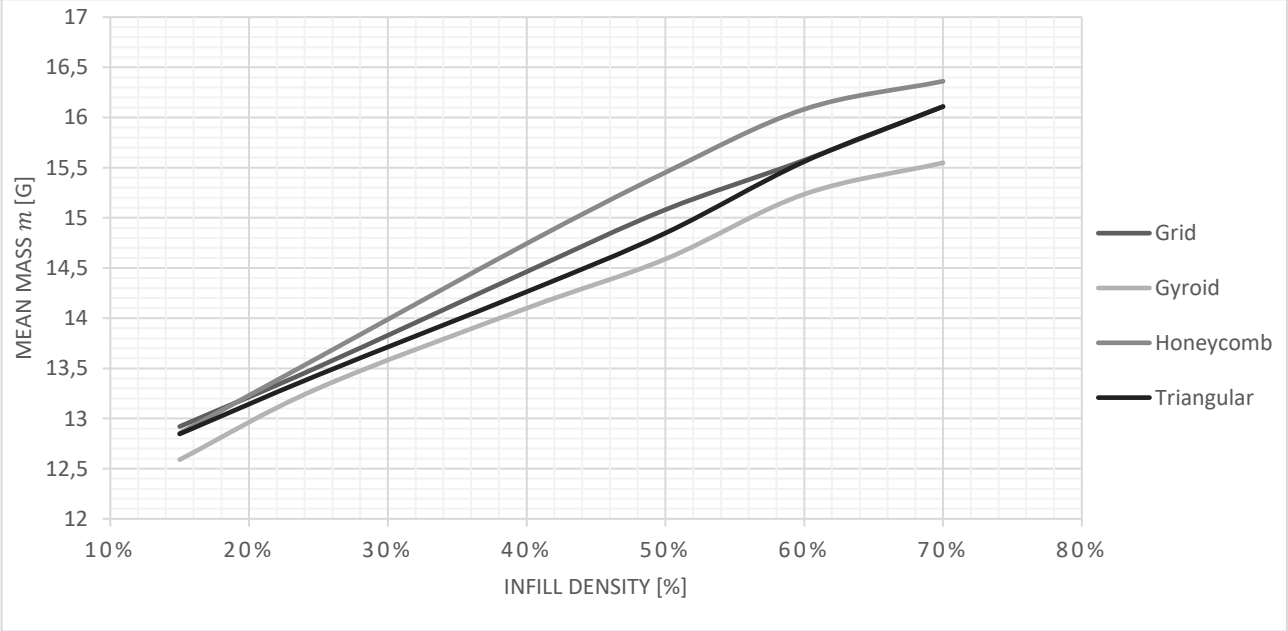

Fig. 5 *PLA – Mean mass of replicas as a function of infill density (Grid, Gyroid, Honeycomb, Triangular).*

Note: Error bars (SD) are not shown in the graphs because the standard deviations are very small across all groups and would be visually negligible at the given scale; the exact mean ± SD values are provided in Table 2.

Figure 5 shows that the mean mass of PLA replicas increases with infill density for all investigated infill patterns, while also highlighting differences among the individual topologies at the same nominal density. The highest values are generally observed for the Honeycomb pattern, whereas lower values are typically associated with Gyroid and Grid. The Triangular pattern lies between these extremes depending on the selected infill density.

3.4 Effect of infill density and infill pattern on the mass of PETG replicas

The same monotonic increase in mass with increasing infill density was confirmed for PETG replicas (Table 2). At 15% infill, masses ranged from 12.996 to 13.641 g, and at 70% infill from 16.258 to 16.855 g.

Compared with PLA, PETG masses were generally higher, which is consistent with PETG's higher material density. The results also indicate that the primary parameter governing replica mass is the selected relative infill density, while the infill pattern has a secondary (yet measurable) effect.

Regarding infill pattern, Gyroid yielded the lowest mass for PETG as well (e.g., 70%: 16.258 g), whereas Honeycomb was associated with the highest masses (e.g., 70%: 16.855 g; Table 2).

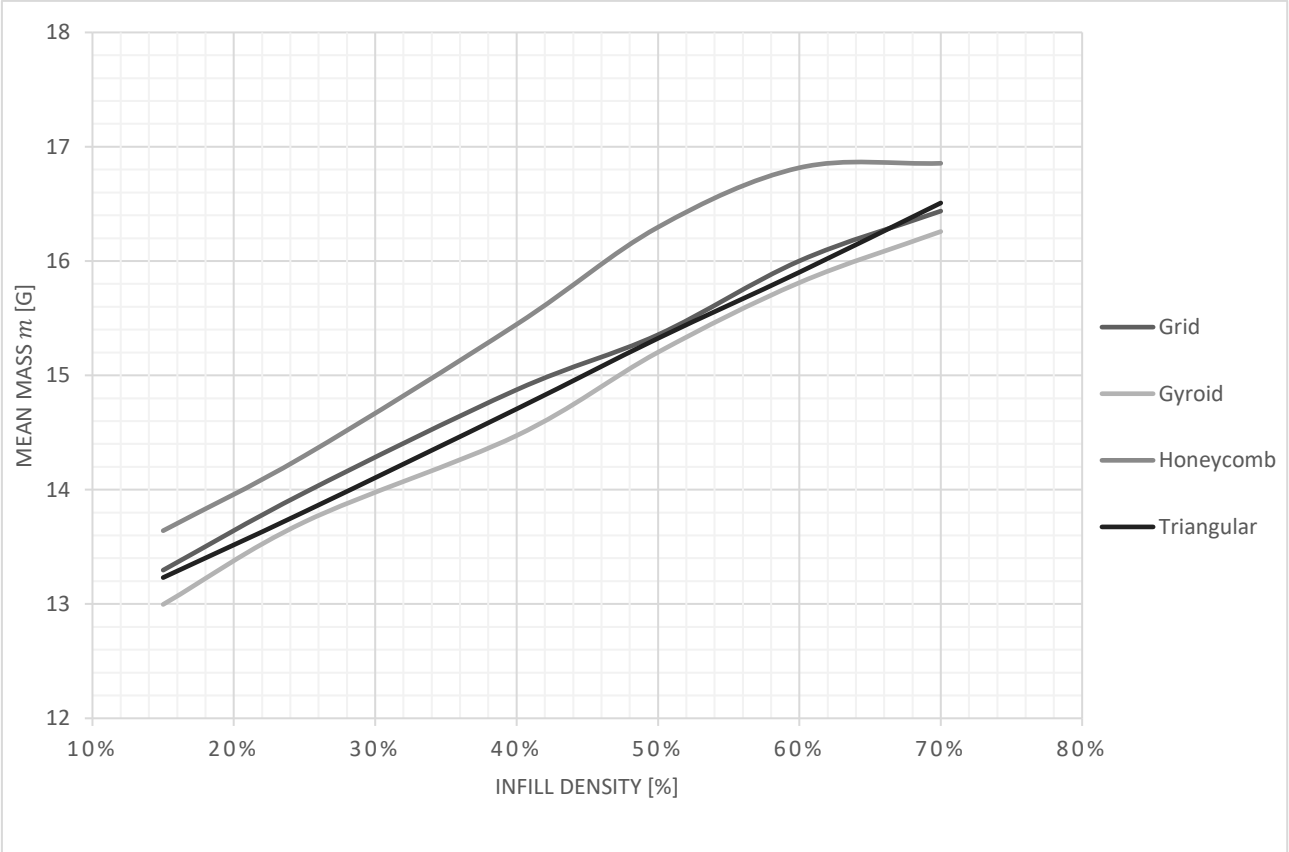

Fig. 6 *PETG – Mean mass of replicas as a function of infill density (Grid, Gyroid, Honeycomb, Triangular).*

Note: Error bars (SD) are not shown in the graphs because the standard deviations are very small across all groups and would be visually negligible at the given scale; the exact mean ± SD values are provided in Table 2.

Figure 6 shows that the mean mass of PETG replicas increases with infill density for all investigated infill patterns and confirms that the resulting mass is influenced not only by infill density but also by infill topology.

The highest values are generally observed for the Honeycomb pattern, whereas lower values are typically associated with Gyroid, Grid, and Triangular. The trends of these three patterns are relatively similar, although measurable differences remain present across the investigated infill densities.

3.5 Overall comparison of PLA vs. PETG and identification of mass-efficient configurations

Overall results for all combinations of material, infill density, and infill pattern are summarized in Table 2. Across both materials, Gyroid is the most mass-efficient pattern, while Honeycomb typically results in the highest mass. The difference between the lightest and heaviest pattern at the same infill density can reach approximately 0.5–0.8 g (e.g., at 70%: PLA 15.548 g vs. 16.361 g; PETG 16.258 g vs. 16.855 g; Table 2).

From a practical school-use perspective, where the goal is to reduce material consumption while maintaining functional usability, configurations in the 40–50% infill range represent a reasonable compromise between mass and expected mechanical robustness. In this range, masses are approximately 14.099–15.452 g (PLA) and 14.473–16.296 g (PETG), depending on the infill pattern (Table 2).

Tab. 2 *Summary of mass results (mean ± SD; n = 15) for the original part and FDM replicas by material, infill density, and infill pattern*

Material	Infill density	Grid	Gyroid	Honeycomb	Triangular
ORG Part	-	11.349±0.013 g			
PLA	15%	12.920±0.023 g	12.590±0.013 g	12.853±0.006 g	12.846±0.008 g
PETG	15%	13.296±0.004 g	12.996±0.005 g	13.641±0.008 g	13.231±0.002 g
PLA	25%	13.515±0.023 g	13.302±0.016 g	13.608±0.007 g	13.435±0.006 g
PETG	25%	13.974±0.028 g	13.718±0.009 g	14.297±0.013 g	13.807±0.002 g
PLA	40%	14.463±0.014 g	14.099±0.018 g	14.743±0.011 g	14.263±0.005 g
PETG	40%	14.874±0.034 g	14.473±0.013 g	15.446±0.010 g	14.706±0.004 g
PLA	50%	15.081±0.007 g	14.589±0.017 g	15.452±0.003 g	14.848±0.002 g
PETG	50%	15.355±0.007 g	15.202±0.015 g	16.296±0.016 g	15.324±0.004 g
PLA	60%	15.574±0.018 g	15.235±0.003 g	16.082±0.005 g	15.560±0.003 g
PETG	60%	16.001±0.002 g	15.811±0.006 g	16.816±0.007 g	15.902±0.004 g
PLA	70%	16.110±0.009 g	15.548±0.020 g	16.361±0.003 g	16.108±0.006 g
PETG	70%	16.437±0.028 g	16.258±0.032 g	16.855±0.008 g	16.508±0.003 g

Note: The reported values represent mean weights in grams expressed as mean ± SD, where SD denotes the standard deviation and n = 15 the number of measured specimens in each group. ORG denotes the original VEX IQ 2×12 Beam part (228 2500 026), which was used as the reference weight m_0 for the calculation of the absolute weight increase according to Equation (1) and the relative weight increase according to Equation (2).

4 Discussion

This study investigated how infill density and infill pattern (Grid, Gyroid, Honeycomb, Triangular) affect the mass of FDM-printed replicas of the VEX IQ 2×12 Beam (228-2500-026), produced from PLA and PETG. The reference mass of the original part was determined by measuring n = 15 pieces, resulting in a mean mass of 11.349 ± 0.013 g. This value was used as the reference level m_0 for evaluating both the absolute mass increase Δm and the relative mass increase Δm_r, enabling direct comparison between the original part and all printed configurations.

4.1 Infill density as the dominant driver of mass

Across all tested patterns and both materials, the results show a clear monotonic increase in mass with increasing infill density. For PLA, mean masses ranged from 12.590–12.920 g at 15 % infill (approximately +10.9 to +13.8 % relative to the original) and increased to 15.548–16.361 g at 70 % infill (approximately +37.0 to +44.2 %). PETG exhibited the same trend (15 %: 12.996–13.641 g; 70 %: 16.258–16.855 g), confirming that the selected infill density is the primary "control parameter" for managing replica mass and, by implication, material consumption when external geometry is kept constant.

From a practical perspective, especially in a school environment where both robustness and material efficiency matter, mid-range infill densities appear to provide a reasonable compromise. In the 40–50 % range, the measured masses were approximately 14.099–15.452 g for PLA and 14.473–16.296 g for PETG, depending on the infill pattern. These values support the idea that substantial reductions in mass (and material use) can be achieved by selecting moderate infill levels rather than maximizing infill density by default.

4.2 Infill pattern as a secondary but measurable factor

Although infill density dominates, the infill pattern produced consistent, measurable differences in mass at the same nominal density. Across both materials, Gyroid repeatedly appeared as the most mass-efficient pattern, while Honeycomb typically resulted in the highest masses. The difference between the lightest and heaviest pattern at the same density reached approximately 0.5–0.8 g (e.g., at 70%: PLA 15.548 g vs. 16.361 g; PETG 16.258 g vs. 16.855 g). While these differences are smaller than those caused by changing infill density, they can still be practically relevant—especially when multiple parts are printed and the mass differences accumulate at the assembly level.

A plausible explanation is that different patterns generate different internal toolpath geometries (total extrusion path length, number of junctions, and local overlap), meaning that the same nominal infill percentage does not necessarily correspond to exactly the same deposited material volume across patterns. Therefore, "infill density" alone may not fully predict mass unless the infill pattern is also specified.

4.3 PLA versus PETG

PETG replicas were generally heavier than PLA replicas across comparable configurations, which is consistent with the higher density of PETG. Importantly, however, the overall behavior remained the same for both materials: infill density was the main determinant of mass, and infill pattern introduced a secondary shift, with Gyroid typically minimizing and Honeycomb typically maximizing the resulting mass.

4.4 Repeatability and interpretation of variability

The standard deviations reported in Table 2 are very small for all groups (n = 15 per group), indicating good repeatability of both the printing process and the weighing procedure. This supports interpreting the observed differences in mean mass as systematic effects driven by the experimental factors (density and pattern), rather than random measurement noise. For this reason, error bars (SD) were omitted from the graphs because they would be visually negligible at the chosen scale; nevertheless, exact mean ± SD values are provided in Table 2 for transparency.

4.5 Link to real-world school testing

The school-based practical testing complements the mass analysis by confirming the functional usability and compatibility of the printed parts, including fit with original components, reliable connections, stability in assemblies, and no restriction of moving elements. In practice, heavier configurations with higher infill densities sometimes contributed positively to the stability of robot models, for example by reducing the tendency to tip over or slip.

Within the scope of school-based practical observations, no clearly negative effect of increased mass on battery life was identified. This suggests that mass optimization in educational robotics should not be interpreted solely as an effort to minimize weight at all costs, but rather as a trade-off among material consumption, robustness, and the stability of the final robot assembly.

4.6 Limitations and recommendations for future work

This work focused primarily on mass. Although practical observations indicated that more robust, and often heavier, configurations were preferred by students and were less prone to damage during handling, mechanical performance was not quantified using standardized destructive testing. The results therefore support conclusions regarding mass, repeatability, and practical usability, but they do not directly establish the optimal configuration in terms of strength, stiffness, or fatigue resistance.

In addition, the absolute mass values are specific to the tested geometry (2×12 Beam) and to the applied printing and slicer settings. Changes in the number of perimeters, top and bottom layers, flow settings, or infill generation strategy may shift the measured values.

For a more comprehensive decision basis in school practice, future work could include: (1) print time and filament consumption, (2) simple application-relevant mechanical tests, such as repeated pin insertion and removal, bending near holes, or failure under prying, and (3) a more quantitative evaluation of stability benefits at the robot level, for example by tilt-angle tipping tests.

Overall, the findings demonstrate that replica mass can be controlled reliably primarily through infill density, while infill pattern provides an additional optimization layer. For educational applications aiming to reduce material consumption while maintaining practical usability, mid-range infill densities (approximately 40–50%) combined with the Gyroid pattern appear to be a mass-efficient choice. Higher infill levels may nevertheless be selected intentionally when increased stability and robustness are prioritized.

5 Conclusions

The aim of this work was to verify the practical usability of FDM-printed replicas of the VEX IQ 2×12 Beam (228-2500-026) in a school environment and to quantify how material (PLA, PETG), infill pattern (Grid, Gyroid, Honeycomb, Triangular), and infill density (15–70%) influence the resulting part mass. Based on the mass measurements (735 pieces in total; n = 15 per group) and the real-world school testing, the following conclusions can be drawn:

- The reference mass of the original part was determined from 15 pieces as 11.349 ± 0.013 g, and this value was used as the reference level m_0 for evaluating both absolute and relative mass increase.
- Infill density is the primary factor controlling replica mass. For both materials and all patterns, a clear monotonic increase in mass with increasing infill density (15–70 %) was confirmed.
- For PLA, masses ranged from 12.590–12.920 g at 15 % infill (approximately +10.9 to +13.8 % relative to the original) and increased to 15.548–16.361 g at 70 % infill (approximately +37.0 to +44.2 %).
- For PETG, masses ranged from 12.996–13.641 g at 15 % infill and reached 16.258–16.855 g at 70 % infill. PETG replicas were

generally heavier than PLA replicas, which is consistent with the higher density of PETG.

- Infill pattern has a secondary but measurable effect. Across both materials, Gyroid repeatedly produced the lowest masses, while Honeycomb typically produced the highest masses. The difference between the lightest and heaviest pattern at the same density reached approximately 0.5–0.8 g (e.g., at 70 %: PLA 15.548 g vs. 16.361 g; PETG 16.258 g vs. 16.855 g).
- Measurement repeatability was high. The standard deviations were very small in all groups, indicating stable printing and weighing and enabling reliable comparisons of mean masses.
- Real-world school testing confirmed functionality and compatibility. The printed parts fit the original system, enabled reliable connections, and were usable by students during assembly and disassembly. In practice, higher infill densities often improved perceived robustness and, in some robot assemblies, contributed positively to stability (e.g., reduced tipping or slipping tendency).
- The increased mass did not show a clearly negative impact on battery life under typical school conditions; differences in operating time per charge were evaluated as negligible.
- Practical recommendation for schools: when the goal is to reduce material consumption while maintaining functional usability, mid-range infill densities (approximately 40–50%) combined with Gyroid appear to be a mass-efficient choice; higher infill densities may be selected intentionally when stability and robustness are prioritized.

Overall, the results show that the mass of FDM replicas can be controlled reliably primarily through infill density, while infill pattern provides an additional fine-tuning option.

Acknowledgement

This article was supported by the SGS grant of J. E. Purkyne University in Usti nad Labem, project No. UJEP-SGS-2025-48-001-1, and by the project DigiLab SMART III – Ustecky kraj, registration number CZ.02.01.02/00/22_009/0004316, implemented within the OP JAK programme.

References

[1] CHACÓN, J.M., CAMINERO, M.A., GARCÍA-PLAZA, E., NÚÑEZ, P.J. (2017). Additive manufacturing of PLA parts by fused deposition modeling: Effect of process parameters on mechanical properties. In: *Materials & Design*, Vol. 124, pp. 143 – 157. DOI 10.1016/j.matdes.2017.03.065

[2] NICOLAU, A., BABA, M.N., CERBU, C., CIOACĂ, C., BRENCI, L.-M., COSEREANU, C. (2025). Evaluation of 3D-Printed Connectors in Chair Construction: A Comparative Study with Traditional Mortise-and-Tenon Joints. In: *Materials*, Vol. 18, No. 1, pp. 201. DOI 10.3390/ma18010201

[3] ZIEMIAN, C.W., ZIEMIAN, S., HAILE, K. (2012). *Characterization of stiffness and strength of FDM manufactured parts*. In: *Rapid Prototyping Journal*, Vol. 18, No. 2, pp. 131 – 143. DOI 10.1108/13552541211212196

[4] FALES, A., ČERNOHLÁVEK, V., SUSZYNSKI, M., ŠTĚRBA, J., ZDRÁHAL, T., NOCAR, D. (2025). Experimental Measurement and Testing of 3D Printed Parts in Terms of the Material Used. In: *Manufacturing Technology*, pp. 174 – 184. DOI 10.21062/mft.2025.016

[5] MENARGUES, S., NAVAS, J., ESPINOSA, I., BAILE, M. T., VAZ, R. F., PICAS, J. A. (2025). Effect of Additive Manufacturing Parameters on PLA, ABS, and PETG Strength. In: *Processes*, Vol. 13, No. 9, pp. 2733. DOI 10.3390/pr13092733

[6] RISMALIA, M., HIDAJAT, S.C., PERMANA, I.G.R., HADISUJOTO, B., MUSLIMIN, M., TRIAWAN, F. (2019). Infill pattern and density effects on the tensile properties of 3D printed PLA material. In: *Journal of Physics: Conference Series*, Vol. 1402. DOI 10.1088/1742-6596/1402/4/044041

[7] KUMARFESAN, R., KADIRGAMA, K., SAMYKANO, M., HARUN, W.S.W., THIRUGNANASAMBANDAM, A., KANNY, K. (2025). In-Depth Study and Optimization of Process Parameters to Enhance Tensile and Compressive Strengths of PETG in FDM Technology. In: *Journal of Materials Research and Technology*, Vol. 37, pp. 397–416. DOI 10.1016/j.jmrt.2025.06.013

[8] KADHUM, A. H., AL-ZUBAIDI, S., ABDULKAREEM, S. S. (2023). Effect of the Infill Patterns on the Mechanical and Surface Characteristics of 3D Printing of PLA, PLA+

and PETG Materials. In: *ChemEngineering*, Vol. 7, No. 3, pp. 46. DOI 10.3390/chemengineering7030046

[9] BUDZIŃSKI, B., FEDEROWICZ, K. (2025). Evaluation of PLA and PETG as 3D-Printed Reference Materials for Compressive Strength Testing. In: *Materials,* Vol. 18, No. 6, DOI 10.3390/ma18163794

[10] ABUEIDDA, D.W., BAKIR, M., AL-RUB, R.K.A., BERGSTRÖM, J.S., SOBH, N.A., JASIUK, I. (2017). Mechanical properties of 3D printed polymeric cellular materials with triply periodic minimal surface architectures. In: *Materials & Design*, pp. 255 – 267. DOI 10.1016/j.matdes.2017.03.018

[11] FALES, A. (2023). Educational Robotics. In: *Proceedings of the International Conference Experimental and Computational Methods in Engineering*, pp. 169 – 172. Usti nad Labem. ISBN 978-80-7561-411-7

[12] PONIKELSKÝ, J., ZURAVSKY, I., ČERNOHLÁVEK, V., CAIS, J., ŠTĚRBA, J. (2021). Influence of production technology on selected polymer properties. In: *Manufacturing Technology*. Vol. 21, No. 4, pp. 520–530. DOI: 10.21062/mft.2021.051.

[13] ZEIZINGER L, JONÁK M. Weight and price optimization of truss construction with using genetic algorithm. In: *Manufacturing Technology*. 2020;20(2):270-275. doi: 10.21062/mft.2020.030.

[14] ČERNOHLÁVEK, V., ŠTĚRBA, J., SVOBODA, M., ZDRÁHAL, T., SUSZYNSKI, M., CHALUPA, M., KROBOT, Z. Verification of the safety of storing a pair of pressure vessels. In: *Manufacturing Technology*, Vol. 21, No. 6, pp:762 – 773. DOI 10.21062/mft.2021.097

[15] FALES, A.; ČERNOHLÁVEK, V.; ŠTĚRBA, J.; DIAN, M.; SUSZYŃSKI, M.: Innovative Approaches to Material Selection and Testing in Additive Manufacturing. In: *Materials*, 2025, 18, 144. DOI 10.3390/ma18010144

[16] ISSAYEV G, AITMAGANBET A, SHEHAB E, ALI H. Bonding Strength Analysis of Multi-material and Multi-color Specimens Printed with Multi-extrusion Printer. In: *Manufacturing Technology*. 2021;21(5):627-633. doi: 10.21062/mft.2021.072.

[17] PONIKELSKÝ, J.; CHALUPA, M.; ČERNOHLÁVEK, V.; ŠTĚRBA, J. (2024). Force and Pressure Dependent Asymmetric Workspace Research of a Collaborative Robot and Human. In: *Symmetry*, Vol. 16, pp. 131. DOI 10.3390/sym16010131

[18] JIN, F., LU, W., AN, X., ZHU, H., WANG, J. (2024). Mechanical Properties and Compression Performance of 3D Printed HIPS Polymer Lattice Structure. In: *Manufacturing Technology*, Vol. 24, No. 3, pp 378 – 392. DOI 10.21062/mft.2024.054.

[19] SUSZYŃSKI, M.; WIŚNIEWSKI, M.; WOJCIECHOWICZ, K.; TRACZYŃSKI, M.; BUTLEWSKI, M.; ČERNOHLÁVEK, V.; TALAR, R. (2025) Study of Positioning Accuracy Parameters in Selected Configurations of a Modular Industrial Robot – Part 1. In: *Sensors*, Vol. 25, pp. 108. DOI 10.3390/s25010108

[20] DEGANOVÁ L, DEKÝŠ V, SAPIETA M, SAPIETOVÁ A. Ultrasonic-Based Active Thermography for Determining Depth Detection Limits in Onyx Composites. In: *Manufacturing Technology*. 2026;26(1):14-25. doi: 10.21062/mft.2026.003.